RSC Advances

PAPER

View Article Online
View Journal | View Issue

Cite this: *RSC Adv.*, 2022, **12**, 35770

Pyrogallol, Corilagin and Chebulagic acid target the "fuzzy coat" of alpha-synuclein to inhibit the fibrillization of the protein†

Mandar Bopardikar,[a] Sri Rama Koti Ainavarapu *[a] and Ramakrishna V. Hosur*[b]

Received 14th July 2022
Accepted 13th October 2022

DOI: 10.1039/d2ra04358k

rsc.li/rsc-advances

The accumulation of the intrinsically disordered protein alpha-synuclein (αSyn) in the form of insoluble fibrillar aggregates in the central nervous system is linked to a variety of neurodegenerative disorders such as Parkinson's disease, Lewy body dementia, and multiple system atrophy. Here we show that Pyrogallol, Corilagin and Chebulagic acid, compounds containing a different number of catechol rings, are independently capable of delaying and reducing the extent of αSyn fibrillization. The efficiency of inhibition was found to correlate with the number of catechol rings. Further, our NMR studies reveal that these compounds interact with the N-terminal region of αSyn which is unstructured even in the fibrillar form of the protein and is known as the "fuzzy coat" of fibrils. Thus, Corilagin and Chebulagic acid target the fuzzy coat of αSyn and not the amyloid core which is a common target for the inhibition of protein fibrillization. Our results indicate that the N-terminus also plays a key role in the fibrillization of αSyn.

Introduction

Neurodegenerative disorders account for a significant and increasing proportion of deaths and disabilities worldwide. Neurodegenerative disorders such as Parkinson's disease (PD), lewy body dementia (LBD) and multiple system atrophy (MSA) are characterized pathologically by the accumulation of alpha-synuclein (αSyn) protein in the form of insoluble aggregates, known as Lewy Bodies (LB), in the cytoplasm of dopaminergic neurons in the central nervous system.[1–3] Familial early onset PD is linked with the duplication or triplication of the gene encoding αSyn (SNCA).[4] These observations suggest a strong correlation between αSyn fibrillization and the occurrence of neurodegenerative disorders like PD, LBD and MSA which are collectively known as synucleinopathies.

αSyn‡ is an intrinsically disordered protein (IDP) that is made up of 140 amino acid residues.[5] αSyn consists of an amphipathic N-terminal domain (residues 1–60), a hydrophobic central part known as NAC (non-amyloid β component) region (residues 61–95) and an acidic C-terminal region (residues 96–140).[6] Interestingly, the Lewy Body variant of Alzheimer's Disease is characterized by the accumulation of a 35 residues long peptide, with the exact same sequence as that of the NAC region of αSyn, along with amyloid β peptide in the form of cytotoxic insoluble aggregates.[7,8]

There is no preventive therapy available for synucleinopathies as yet. However, inhibition of αSyn fibrillization with the help of chemical reagents represents a likely therapeutic strategy. In the past few years, several studies have reported the inhibition of αSyn fibrillization by small organic molecules,[9–35] nanomaterials,[36–38] herbal formulations[39–43] and chaperone proteins.[44–46] However, there are relatively fewer reports which provide an in-depth residue-level understanding of how these reagents inhibit αSyn fibrillization.[14,15,17,20,45–48] A vast majority of the small organic molecules that are capable of inhibiting αSyn fibrillization are catechols.[9] Here, we have investigated the effect of Pyrogallol (PGL), Corilagin (CLN) and Chebulagic acid (CA) (Fig. 1) on αSyn fibrillization. The choice of these molecules was driven by the presence of different number of catechol rings. PGL, CLN and CA consist of one, three and four catechol

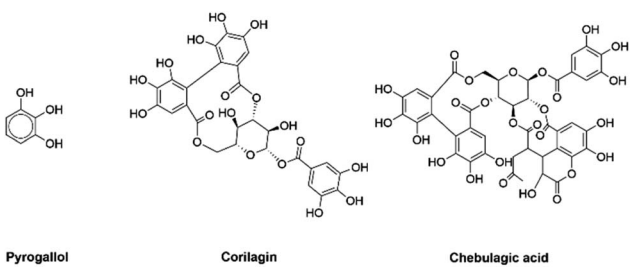

Fig. 1 The chemical structures of Pyrogallol, Corilagin and Chebulagic acid.

[a]*Department of Chemical Sciences, Tata Institute of Fundamental Research, Homi Bhabha Road, Colaba, Mumbai 400005, India. E-mail: koti@tifr.res.in*

[b]*UM-DAE Centre for Excellence in Basic Sciences, University of Mumbai, Kalina Campus, Santacruz, Mumbai 400098, India. E-mail: rvhosur53@gmail.com*

† Electronic supplementary information (ESI) available: Comparison between the electronic absorption profile of ThT and the catechols, Pyrogallol (PGL), Corilagin (CLN) and Chebulagic acid (CA) (Fig. S1), $^{1}H–^{15}N$ HSQC signal attenuation (I/I_0) of αSyn in various conditions (Fig. S2) and statistical analyses of $^{1}H–^{15}N$ HSQC intensity ratios of αSyn (Table S1). See DOI: https://doi.org/10.1039/d2ra04358k

‡ Accession code: alpha-synuclein (*Homo sapiens*) UniProtKB-P37840 (SYUA_HUMAN).

rings respectively. The point here is to understand qualitatively, the dependence of amyloid inhibition potential of catechol compounds on the number of catechol rings. Also, in a previous study we had shown that triphala, a herbal preparation, is effective in inhibiting αSyn fibrillization and that PGL, CLN and CA are ingredients of triphala.[39] Therefore, in the current study we wanted to investigate the effect of each of these molecules on αSyn fibrillization.

PGL is known to possess antiproliferative activity towards human tumor cell lines.[49] Also, it has been reported that PGL induces G2-M arrest in human lung cancer cells and inhibits tumor growth in animal model system.[50] Another study has shown that PGL regulates expression of pro-inflammatory genes in bronchial epithelial cells.[51] On the other hand, CLN is capable of alleviating hepatic fibrosis caused by egg granuloma in *Schistosoma japonicum* infection.[52] A study has shown that CLN exhibits anti-hyperalgesic activity in thermal and chemical stimulation cased nociception mice models.[53] It has been demonstrated that CLN produces anti-inflammatory effect in herpes simplex virus (HSV)-1 induced encephalitis.[54] In the case of CA, it is known that this compound exerts inhibitory effect on neuraminidase-mediated influenza A viral release[55] and also possesses broad-spectrum antiviral activity against viruses that use glycosaminoglycans for entry.[56] CA inhibits tumor necrosis factor-α induced pro-angiogenic and pro-inflammatory activities in retinal capillary endothelial cells by inhibiting the phosphorylation of p38 group of mitogen-activated protein (MAP) kinases, extracellular signal-regulated kinase (ERK) and nuclear factor kappa-light-chain-enhancer of activated B cells (NFκB).[57] CA is a highly potent inhibitor of topoisomerase I.[58]

As mentioned above, there are several reports showing the therapeutic potential of PGL, CLN and CA against different disorders and infections. However, the effect of these compounds on αSyn fibrillization has not been studied so far. In the current study, we find that they are independently capable of delaying and reducing the extent of fibrillization of αSyn. Further, our NMR studies provide residue-level insights into the mode of interaction of these compounds with αSyn.

Materials and methods

Protein overexpression and purification

αSyn gene inserted into a pT7-7 vector construct, with the capability to withstand ampicillin, was expressed in *Escherichia coli* (*E. coli*) BL21 (DE3) cells. A glycerol stock of these *E. coli* cells, containing αSyn plasmid, was inoculated into 10 ml of LB containing 100 μg ml^{-1} of freshly prepared ampicillin. The culture was allowed to grow overnight at 37 °C with shaking (180 rpm). The overnight culture was then transferred to 1 litre of LB or M9 culture containing 100 μg ml^{-1} ampicillin. The resulting culture was grown until an OD_{600} of 0.8–1.0 was reached. At this point, the culture was instigated for protein expression with the help of 1 mM IPTG for 6–10 h. Eventually, the cells were pelleted down from the culture and then stored at −80 °C. αSyn protein was purified by a method reported earlier.[59,60] The method goes as follows: initially, frozen cell pellet obtained from 1 litre culture was resuspended in Tris buffer (50 mM Tris, 10 mM EDTA and 150 mM NaCl) pH 8. Subsequently, sonication was performed for 10 min. Then, the suspension was placed in a boiling water-bath for 20 min. This was followed by centrifugation for 10 min. After centrifugation, the precipitate was discarded and the supernatant was collected into a fresh tube. Streptomycin sulphate (136 μl of 10% solution per ml of supernatant) and glacial acetic acid (228 μl per ml of supernatant) were added to the supernatant. The resulting mixture was centrifuged for 10 min. Again, the supernatant was collected, whereas, the precipitate was discarded. Now, saturated ammonium sulphate was added to the supernatant in 1 : 1 (v/v) proportion which causes protein precipitation. Precipitated protein was washed with ammonium sulphate solution (50% saturated). The pellet was resuspended in 3 ml of 100 mM ammonium acetate and re-precipitated with the help of an equal volume of ethanol. The previous step was performed a total of three times. The precipitate was then solubilized in 100 mM ammonium acetate. Ultimately, the solution was frozen in liquid nitrogen and lyophilized. Prior to usage in experiments, the lyophilized protein was further purified by solubilizing it in PBS (10 mM Na_2HPO_4, 1.8 mM KH_2PO_4, 137 mM NaCl, 2.7 mM KCl and 0.01% (w/v) sodium azide) pH 7.4, followed by centrifugation and then performing size exclusion chromatography for the supernatant using a HiLoad 16/600 Superdex75 column (GE Healthcare, UK) with the help of BioLogic DuoFlow FPLC system (Bio-Rad, USA). The protein purity of the fractions was analyzed by SDS-PAGE. All of those fractions which contained only pure αSyn were pooled together and concentrated with the help of 3 kDa Amicon ultra centrifugal filter units (Merck KGaA, Germany). Protein concentration was determined spectrophotometrically by UV absorption measurements using $\varepsilon_{280} = 5960\ M^{-1}\ cm^{-1}$.

Thioflavin T (ThT) fluorescence assay

The process of fibrillization was initiated with 150 μM αSyn in 2 ml Protein LoBind Eppendorf tube in PBS pH 7.4. The protein samples either in the presence or absence of equimolar concentration of PGL, CLN or CA were exposed to mechanical agitation at 65 rpm and 37 °C. At different time points, 5 μl aliquots were taken out from each of the samples. Each aliquot was added to 245 μl of 15 μM ThT solution in PBS pH 7.4. Fluorescence was immediately recorded for the resulting solution with an Agilent spectrofluorometer. The excitation wavelength and emission wavelength range were 444 nm and 455–500 nm respectively. For all the measurements, both the excitation and emission bandwidths were 5 nm. In the end, the normalized fluorescence intensity at 485 nm was plotted against time.

ThT fluorescence data analysis

The ThT fluorescence data sets reporting the fibrillization of αSyn in the absence and presence of PGL or CLN were fitted with the following equation:

$$y(t) = A + \frac{B - A}{1 + \exp\left(-k\left(t - T_{\text{half}}\right)\right)} \quad (1)$$

where 'y' is normalized ThT fluorescence intensity at time 't'. T_{half} represents the inflection point for the sigmoidal function (eqn (1)). T_{half} is also the time required to reach 50% of maximal fluorescence. B and A represent maximum and minimum ThT fluorescence respectively. The duration of lag phase (T_{lag}) was calculated as follows:

$$T_{lag} = T_{half} - 2/k \quad (2)$$

All the data analysis was performed with the help of in-house written python programs.

Transmission electron microscopy (TEM)

At the end of the fibrillization process, each sample was diluted to 30 μM with 0.22 micron filtered distilled water. These samples were then spotted onto a carbon-coated Formvar grid and incubated for 5 min. Further, staining was performed with a freshly prepared 1% (w/v) aqueous solution of uranyl acetate, filtered through 0.22 μm syringe filter, by incubation for 1 min. Eventually, the samples were washed with 0.22 micron filtered distilled water. The samples were then allowed to dry overnight. Finally, images were acquired using a 200 kV FEI Tecnai-20 transmission electron microscope (TEM).

Nuclear magnetic resonance (NMR) spectroscopy

NMR experiments were performed on 800 MHz Bruker Avance NMR spectrometer equipped with cryogenically cooled triple-resonance probe. All the NMR measurements were performed in PBS, pH 7.4 at a temperature of 280 K if not otherwise indicated. ^{1}H–^{15}N BEST-HSQC spectra were recorded for 108 μM ^{15}N isotopically enriched αSyn in the presence and absence of different concentrations of PGL, CLN or CA with inter-scan delays of 200 ms and 2048 × 512 points for the ^{1}H and ^{15}N dimension respectively. Spectra were recorded in phase-sensitive mode and quadrature detection was performed with the help of States-TPPI method.[61] The ^{1}H and ^{15}N dimensions were zero-filled to 4096 and 1024 points, respectively. Sine squared bell apodization with SSB = 2 was used as a window function for both dimensions. Data was processed with the help of Topspin 4.0 (Bruker, USA) and analysed with CCPN[62] (Collaborative Computing Project for NMR, University of Leicester, UK). Chemical shift assignments were obtained by transfer from BMRB (accession number 16300) and other previous reports.[46] Chemical shift perturbations (CSP) were calculated as $\left((\Delta H)^2 + \left(\frac{\Delta N}{5}\right)^2\right)$ where ΔN and ΔH represent the difference in the nitrogen and proton chemical shifts of αSyn in the presence of PGL, CLN or CA with respect to that of pure αSyn, respectively.

Results and discussion

Pyrogallol, Corilagin and Chebulagic acid inhibit αSyn fibrillization

The process of fibrillization of αSyn was monitored with the help of thioflavin T (ThT) binding assay[63–65] in a time-dependent manner. αSyn fibrillization is a nucleation-controlled polymerization[66] process which shows a sigmoidal curve with three different phases – (i) nucleation or lag, (ii) elongation and (iii) saturation. It was observed that an equimolar concentration of PGL or CLN increased the duration of the nucleation phase or lag phase (Fig. 2(A)). In other words, both PGL and CLN delayed the onset of αSyn fibrillization. Also, there was reduction in ThT fluorescence in the saturation phase to 52% and 13% in the presence of PGL and CLN, respectively (Fig. 2(A)), indicating that a smaller amount of the protein underwent the transition from natively unstructured conformation into the amyloid fibrillar form as compared to the protein in the absence of these molecules. In order to check for any interfering effects of PGL, CLN or CA on the ThT fluorescence assay due to (a) absorbance in the wavelength region where ThT fluoresces or (b) absorbance in the wavelength region where ThT absorbs, UV-visible spectrophotometric measurements were performed (see ESI Methods). It was observed that PGL, CLN or CA do not absorb in this spectral region (Fig. S1†). Therefore, the reduced ThT fluorescence (Fig. 2(A)) may be attributed to the inhibition of αSyn fibrillization by PGL, CLN or CA in the respective cases.

Further quantitative insights into the effect of PGL and CLN on αSyn fibrillization were obtained by fitting the ThT data sets with sigmoidal function (eqn (1) in Materials and Methods) to obtain the values of some of the important parameters (eqn (2) in Materials and Methods) characterizing the process of amyloid formation – duration of lag phase (T_{lag}), inflection point (T_{half}) which is also the time required to reach 50% of maximal fluorescence and apparent first-order rate constant (k). For αSyn alone, T_{lag} was 38 (h) (Fig. 2(B) and Table 1). In the presence of PGL and CLN, the value of T_{lag} increased to 112 (h) and 86 (h) respectively (Fig. 2(B) and Table 1). Thus, the presence of PGL and CLN clearly caused a delay in the initiation of αSyn fibrillization. On the other hand, the value of k was 0.25 (h^{-1}) for αSyn, which decreased to 0.13 (h^{-1}) and 0.047 (h^{-1}) in the presence of PGL and CLN respectively (Fig. 2(C) and Table 1). This shows that PGL reduced the rate of αSyn fibrillization to nearly half its value,

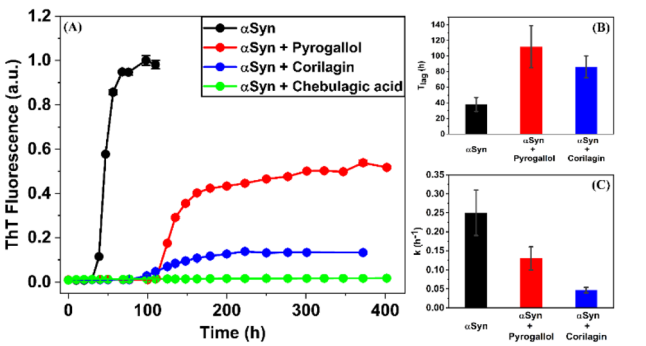

Fig. 2 Effect of Pyrogallol, Corilagin or Chebulagic acid on αSyn fibrillization. (A) Normalized ThT fluorescence reporting αSyn fibrillization in the absence (black) and presence of equimolar concentration of Pyrogallol (red), Corilagin (blue) or Chebulagic acid (green). Duration of lag phase (B) and apparent first-order rate constant (C) for αSyn fibrillization in the absence (black) and presence of Pyrogallol (red) and Corilagin (blue).

Table 1 Parameters[a] for αSyn fibrillization in absence and presence of Pyrogallol or Corilagin as monitored by ThT fluorescence

Experiment	T_{lag} (h)	T_{half} (h)	k (h^{-1})
αSyn	38 ± 9	45.8 ± 0.9	0.25 ± 0.06
αSyn + Pyrogallol	112 ± 27	127 ± 2	0.13 ± 0.03
αSyn + Corilagin	86 ± 14	128 ± 3	0.047 ± 0.007
αSyn + Chebulagic acid	—	—	—

[a] Values of parameters in Table 1 were obtained by fitting the data in Fig. 2(A) with eqn (1) and T_{lag} was calculated with the help of eqn (2). The errors represent twice the standard deviation (2σ) from the mean.

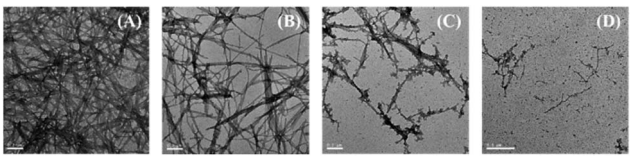

Fig. 3 TEM images at the end of the αSyn fibrillization process in the absence (A) and presence of equimolar concentration of Pyrogallol (B), Corilagin (C) and Chebulagic acid (D). Scale bar represents 200 nm for (A), (B), (C) and 500 nm for (D).

whereas, CLN caused more than five times reduction. In the case of CA, the efficiency of inhibition was so high that there was no observable increase in ThT fluorescence even up to 17 days of incubation. Our ThT fluorescence experiments suggest that the efficiency of these compounds to inhibit αSyn fibrillization is in the following order:

Chebulagic acid > Corilagin > Pyrogallol.

In order to confirm these observations, transmission electron microscopy (TEM) studies were performed to assess the effect of these compounds on αSyn fibril morphology and density. It was observed that PGL, CLN and CA cause a decrease in the fibril density (Fig. 3). However, the most pronounced effect was observed in the case of CA, where the reduction in fibril density was highest (Fig. 3). Thus, our TEM studies qualitatively support the trend shown by ThT fluorescence data.

Corilgain and Chebulagic acid mainly interact with the N-terminal region of αSyn

In order to understand the mechanism of inhibition of αSyn fibrillization by PGL, CLN and CA, ^{1}H–^{15}N HSQC experiments were performed on uniformly ^{15}N isotopically enriched protein in the absence and presence of each of these compounds. However, before we understand the nature of interaction of these amyloid inhibitors with αSyn by NMR, it is important to note that the addition of each of these molecules to PBS solution introduced pH changes. It was observed the pH difference between the 'protein + ligand' solution and the protein solution was ~0.3, ~0.5 and ~0.7 in the case of PGL, CLN and CA respectively (Fig. S2†). Now it is possible that such a pH change in the solution conditions might affect the NMR intensities and thereby interfere with the experiment. Upon investigation, we indeed observed a drastic deviation in the intensities of αSyn peaks when the pH of the 'protein + ligand' solution and the protein solution was not adjusted to the same value as compared to when there was no pH difference between these two solutions (Fig. S2†). Interestingly, even a pH change, as small as 0.3 (in the case of PGL) was found to have a profound influence on the intensities of ^{1}H–^{15}N resonances of αSyn (Fig. S2(A) and (B)†). This shows that protein backbone resonances could be extremely sensitive to the solvent conditions, especially pH which is possibly due to the labile nature of the backbone amide protons. Therefore, all our NMR experiments were performed with utmost care taking into consideration these drastic effects of pH conditions.

An overlay of the two-dimensional NMR spectra of αSyn in the absence and presence of each amyloid inhibitor provided crucial insight into the location of residues that were affected the most by that particular compound (Fig. 4). It was observed that most of these residues belonged to the N-terminus in all the three cases (Fig. 4(A–C)). In order to obtain further insight, the intensity ratio and CSP for each individual well-resolved resonance were calculated for αSyn in the presence of each compound and plotted against the corresponding residue position in the protein primary sequence (Fig. 5). When equimolar amounts of PGL were used, the peak intensities were unaffected (Fig. 5(A)). However, when five molar equivalent concentration of PGL was used, peak broadening was observed for residues in the N-terminal domain and NAC region (Fig. 5(A)). The peak intensities dropped to nearly 83% in these domains of αSyn (Fig. 5(A) and Table S1†). This observation suggests that it is the N-terminal domain and NAC region of the protein which interact with PGL.

In the case of CLN, similar peak broadening was observed in the N-terminus and NAC domain when five molar equivalent

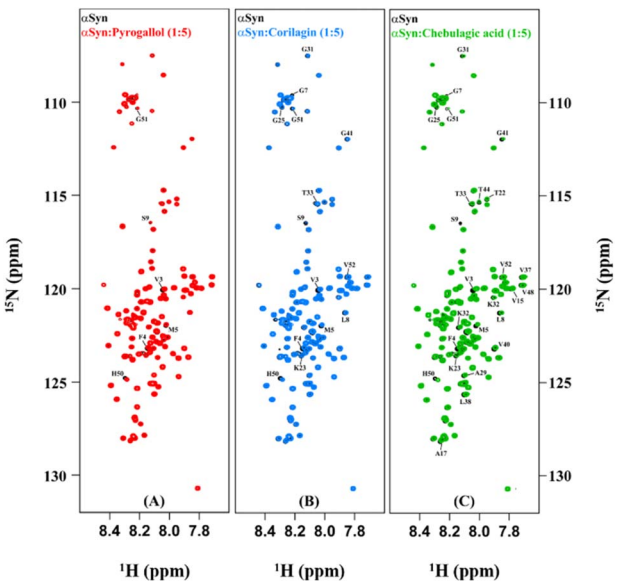

Fig. 4 Residue-level insights into the interaction of αSyn with the amyloid inhibitors. Overlay of two-dimensional ^{1}H–^{15}N HSQC spectra of 108 μM αSyn in the absence (black) and presence of 540 μM of Pyrogallol (red), Corilagin (blue) and Chebulagic acid (green) is shown in (A), (B) and (C) respectively.

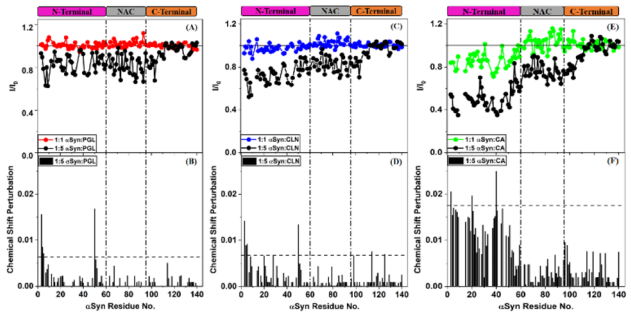

Fig. 5 Corilagin and Chebulagic acid mainly interact with the N-terminal region of αSyn. (A, C and E) $^{1}H-^{15}N$ HSQC signal attenuation of αSyn in the presence of Pyrogallol (PGL), Corilagin (CLN) and Chebulagic acid (CA) respectively. The horizontal solid line in (A), (C) and (E) indicates an I/I_0 ratio of 1. (B, D and F) CSP values for αSyn in the presence of five equivalents of PGL, CLN and CA respectively. The horizontal dashed line in (B), (D) and (F) indicates twice the standard deviation (2σ) above the mean. The vertical dash-dotted lines across (A and B), (C and D) and (E and F) mark the different domains of αSyn.

concentration of CLN was used (Fig. 5(C)). However, the reduction in intensities for N-terminus was to a higher extent up to 73% as compared to NAC region 82% (Fig. 5(C) and Table S1†). The extent of signal attenuation for N-terminal region was found to be statistically higher than NAC domain (Table S1†). This suggests that the N-terminus is a preferred interaction domain for CLN over the NAC region of αSyn. The small magnitude of CSPs (<0.01 ppm) in the presence of PGL and CLN (Fig. 5(B) and (D)) is suggestive of the weak and transient nature of the interactions between each of these molecules and the protein.

On the other hand, the addition of equimolar amount of CA to αSyn resulted in a slight reduction in intensity for N-terminal residues (Fig. 5(E)). At a higher concentration of CA, that is αSyn : CA 1 : 5 molar stoichiometry, a drastic reduction in the peak intensities for residues in the N-terminus was observed (Fig. 5(E)). In fact, intensity ratios dropped to nearly 50% for residues V3-V26 and A29-G51 (Fig. 5(E)). The average signal attenuation of 51% for N-terminus was found to be statistically much lower (Table S1†) as compared to 76% for NAC region (Fig. 5(E) and Table S1†) indicating that CA prefers interaction with N-terminal region over NAC domain. Clearly, the effect of CA was much more pronounced as compared to that of PGL and CLN. Also, the CSPs were higher in the case of CA (Fig. 5(F)) in comparison to those observed due to PGL and CLN (Fig. 5(B) and (D) respectively).

Significance of the disordered N-terminus of αSyn in the process of fibrillization

Protein fibrillization is a complex and heterogeneous process. During this process, monomeric protein self-assembles along a multitude of pathways to form a wide variety of species such as off-pathway oligomers, on-pathway oligomers that transform into fibrils in the due course of time, protofibrils and fibrils. In the case of αSyn, the fibrillar core consists of a rigid Greek-key motif which is flanked by the unstructured C- and N-termini.[67,68] Current ways of inhibiting protein fibrillization mainly target the amyloid core and include sequestration of monomers to prevent self-assembly,[69,70] treatment with reagents that cause fibril clustering which reduces fragmentation of fibrils and consequently conceals binding site(s) for the addition of monomeric protein[71,72] and using chaperones or engineered proteins to choke fibril surfaces.[73–75] However, recent years have witnessed a growing interest in understanding the role of unstructured regions in fibril elongation. Truncating the disordered N- and C-termini modulates the aggregation kinetics of αSyn suggesting that these unstructured regions are not mere bystanders but actively participate in the process of fibrillization.[76–79] In fact, Yang *et. al.* showed that the first 11 residues in the unstructured N-terminal region of αSyn form a motif for the recruitment of monomeric protein to fibril.[80]

Here we have shown that Pyrogallol, Corilagin and Chebulagic acid inhibit αSyn fibrillization by interacting with the extreme N-terminal region of the protein. Our results, especially in the case of Chebulagic acid, clearly show that the N-terminus of αSyn plays a crucial role in the process of fibrillization of the protein. Similar to our findings, Burmann *et. al.* had observed that six different chaperone proteins inhibit αSyn fibrillization by binding to a common motif consisting of 12 residues in the N-terminus.[46] Also, a recent study showed that an off-pathway oligomer of αSyn acts as an auto-inhibitor of fibrillization by recruiting monomeric protein through an N-terminal binding site comprising of the first 11 residues.[80] All of these evidences highlight the significance of the N-terminal domain of αSyn in the process of fibrillization of the protein.

Conclusions

Our results demonstrate that Pyrogallol, Corilagin and Chebulagic acid inhibit αSyn fibrillization. Interestingly, each of these amyloid inhibitors interact with αSyn in the N-terminal and NAC regions of the protein. The C-terminal domain, which is highly acidic in nature, remains unaffected. In the case of Corilagin and Chebulagic acid, the interaction is more pronounced in the N-terminus than the NAC region. Corilagin and Chebulagic acid target the unstructured part of αSyn which belongs to the extreme N-terminal region of the protein, comprising of residues 3–26 and interact relatively weakly with the amyloid core, consisting of residues 37–43, 52–59, 62–66, 68–77 and 90–95, which is a common target for inhibiting fibrillization.[81] Further studies need to be undertaken in order to understand the role of N-terminus in αSyn fibrillization in greater detail which could lead to the development of better therapeutic approaches for amyloid inhibition in the future.

The compounds utilized in this study showed an efficacy to inhibit αSyn fibrillization in the following order: Chebulagic acid > Corilagin > Pyrogallol. Interestingly, the number of catechol rings in these molecules follows the same order, that is, Chebulagic acid, Corilagin and Pyrogallol consist of four, three and one catechol rings respectively. This observation possibly indicates that the capability of catechols to inhibit αSyn fibrillization could be dependent on the number of catechol rings. Further studies investigating the effect of

a systematically designed library of catechols need to be pursued to confirm this observation. On the other hand, the fact that the choice of Pyrogallol, Corilagin and Chebulagic acid was also driven by these compounds being ingredients of triphala, herbal preparation which was previously shown to be effective in inhibiting αSyn fibrillization,[39] strongly suggests that natural product-based drug discovery is an exercise worth perceiving towards the identification of new and effective amyloid inhibitors.

Author contributions

M. B., S. R. K. A. and R. V. H. conceived the project. M. B. performed all the experiments and analyzed the results. M. B. wrote the manuscript. All the authors were involved in the interpretation of results. S. R. K. A. and R. V. H. corrected the manuscript.

Conflicts of interest

There are no conflicts to declare.

Acknowledgements

αSyn plasmid was a kind gift from Prof. Vinod Subramaniam, Vrije Universiteit Amsterdam. The authors are thankful to Shilpa Shirodkar, Jayesh Parmar and Lalit Borde for their help in TEM imaging. The authors are grateful to the National Facility for High-Field NMR at TIFR, Mumbai. The authors would like to thank Sudipta Maiti, Janeka Gartia and Anusri Bhattacharya for discussions during the course of the study. The help received from Ashutosh Kumar and Rajlaxmi Panigrahi in NMR data analysis is highly appreciated. S. R. K. A. acknowledges the financial support of the Department of Atomic Energy (DAE), India under Project No. 12-R&DTFR-5.10-0100.

Notes and references

1 J. Q. Trojanowski, M. Goedert, T. Iwatsubo and V. M. Y. Lee, *Cell Death Differ.*, 1998, **5**, 832–837.
2 M. Hashimoto and E. Masliah, *Brain Pathol.*, 1999, **9**, 707–720.
3 D. M. Skovronsky, V. M. Y. Lee and J. Q. Trojanowski, *Annu. Rev. Pathol.: Mech. Dis.*, 2006, **1**, 151–170.
4 A. B. Singleton, M. Farrer, J. Johnson, A. Singleton, S. Hague, J. Kachergus, M. Hulihan, T. Peuralinna, A. Dutra, R. Nussbaum, S. Lincoln, A. Crawley, M. Hanson, D. Maraganore, C. Adler, M. R. Cookson, M. Muenter, M. Baptista, D. Miller, J. Blancato, J. Hardy and K. Gwinn-Hardy, *Science*, 2003, **302**, 841.
5 P. H. Weinreb, W. Zhen, A. W. Poon, K. A. Conway and P. T. Lansbury Jr, *Biochemistry*, 1996, **35**, 13709–13715.
6 D. J. Moore, A. B. West, V. L. Dawson and T. M. Dawson, *Annu. Rev. Neurosci.*, 2005, **28**, 57–87.
7 K. Uéda, H. Fukushima, E. Masliah, Y. Xia, A. Iwai, M. Yoshimoto, D. A. Otero, J. Kondo, Y. Ihara and T. Saitoh, *Proc. Natl. Acad. Sci. U. S. A.*, 1993, **90**, 11282–11286.
8 O. M. El-Agnaf, R. Jakes, M. D. Curran, D. Middleton, R. Ingenito, E. Bianchi, A. Pessi, D. Neill and A. Wallace, *FEBS Lett.*, 1998, **440**, 71–75.
9 K. A. Conway, J. C. Rochet, R. M. Bieganski and P. T. Lansbury Jr, *Science*, 2001, **294**, 1346–1349.
10 J. Li, M. Zhu, S. Rajamani, V. N. Uversky and A. L. Fink, *Chem. Biol.*, 2004, **11**, 1513–1521.
11 M. Caruana, T. Högen, J. Levin, A. Hillmer, A. Giese and N. Vassallo, *FEBS Lett.*, 2011, **585**, 1113–1120.
12 B. Ahmad and L. J. Lapidus, *J. Biol. Chem.*, 2012, **287**, 9193–9199.
13 M. Zhu, S. Han and A. L. Fink, *Biochim. Biophys. Acta*, 2013, **1830**, 2872–2881.
14 D. E. Ehrnhoefer, J. Bieschke, A. Boeddrich, M. Herbst, L. Masino, R. Lurz, S. Engemann, A. Pastore and E. E. Wanker, *Nat. Struct. Mol. Biol.*, 2008, **15**, 558–566.
15 X. Meng, L. A. Munishkina, A. L. Fink and V. N. Uversky, *Biochemistry*, 2009, **48**, 8206–8224.
16 X. Meng, L. A. Munishkina, A. L. Fink and V. N. Uversky, *Parkinson's Dis.*, 2010, **2010**, 1–16.
17 G. R. Lamberto, A. Binolfi, M. L. Orcellet, C. W. Bertoncini, M. Zweckstetter, C. Griesinger and C. O. Fernandez, *Proc. Natl. Acad. Sci. U. S. A.*, 2009, **106**, 21057–21062.
18 L. Breydo, J. W. Wu and V. N. Uversky, *Biochim. Biophys. Acta*, 2012, **1822**, 261–285.
19 P. K. Singh, V. Kotia, D. Ghosh, G. M. Mohite, A. Kumar and S. K. Maji, ACS Chem, *Neurosci.*, 2013, **4**, 393–407.
20 M. Perni, C. Galvagnion, A. Maltsev, G. Meisl, M. B. Müller, P. K. Challa, J. B. Kirkegaard, P. Flagmeier, S. I. Cohen, R. Cascella, S. W. Chen, R. Limbocker, P. Sormanni, G. T. Heller, F. A. Aprile, N. Cremades, C. Cecchi, F. Chiti, E. A. Nollen, T. P. Knowles, M. Vendruscolo, A. Bax, M. Zasloff and C. M. Dobson, *Proc. Natl. Acad. Sci. U. S. A.*, 2017, **114**, E1009–E1017.
21 N. N. Jha, R. Kumar, R. Panigrahi, A. Navalkar, D. Ghosh, S. Sahay, M. Mondal, A. Kumar and S. K. Maji, ACS Chem, *Neurosci.*, 2017, **8**, 2722–2733.
22 T. Ibrahim and J. McLaurin, *Biochem. Biophys. Res. Commun.*, 2016, **469**, 529–534.
23 A. A. Deeg, A. M. Reiner, F. Schmidt, F. Schueder, S. Ryazanov, V. C. Ruf, K. Giller, S. Becker, A. Leonov, C. Griesinger, A. Giese and W. Zinth, *Biochim. Biophys. Acta*, 2015, **1850**, 1884–1890.
24 N. Ahsan, S. Mishra, M. K. Jain, A. Surolia and S. Gupta, *Sci. Rep.*, 2015, **5**, 9862.
25 K. Ji, Y. Zhao, T. Yu, Z. Wang, H. Gong, X. Yang, Y. Liu and K. Huang, *Food Funct.*, 2016, **7**, 409–416.
26 N. N. Jha, D. Ghosh, S. Das, A. Anoop, R. S. Jacob, P. K. Singh, N. Ayyagari, I. N. Namboothiri and S. K. Maji, *Sci. Rep.*, 2016, **6**, 28511.
27 N. Ahsan, I. A. Siddique, S. Gupta and A. Surolia, *Eur. J. Med. Chem.*, 2018, **143**, 1174–1184.
28 R. Chakraborty, S. Sahoo, N. Halder, H. Rath and K. Chattopadhyay, ACS Chem, *Neurosci.*, 2019, **10**, 573–587.

29 D. Yedlapudi, G. S. Joshi, D. Luo, S. V. Todi and A. K. Dutta, *Sci. Rep.*, 2016, **6**, 38510.
30 J. Pujols, S. Peña-Díaz, D. F. Lázaro, F. Peccati, F. Pinheiro, D. González, A. Carija, S. Navarro, M. Conde-Giménez, J. García, S. Guardiola, E. Giralt, X. Salvatella, J. Sancho, M. Sodupe, T. F. Outeiro, E. Dalfó and S. Ventura, *Proc. Natl. Acad. Sci. U. S. A.*, 2018, **115**, 10481–10486.
31 S. Ghosh, A. Kundu and K. Chattopadhyay, *Sci. Rep.*, 2018, **8**, 5481.
32 D. Ghosh, S. Mehra, S. Sahay, P. K. Singh and S. K. Maji, *Int. J. Biol. Macromol.*, 2017, **100**, 37–54.
33 M. J. Daniels, J. B. Nourse Jr, H. Kim, V. Sainati, M. Schiavina, M. G. Murrali, B. Pan, J. J. Ferrie, C. M. Haney, R. Moons, N. S. Gould, A. Natalello, R. Grandori, F. Sobott, E. J. Petersson, E. Rhoades, R. Pierattelli, I. Felli, V. N. Uversky, K. A. Caldwell, G. A. Caldwell, E. S. Krol and H. Ischiropoulos, *Sci. Rep.*, 2019, **9**, 2937.
34 S. S. Save, K. Rachineni, R. V. Hosur and S. Choudhary, *Int. J. Biol. Macromol.*, 2019, **141**, 585–595.
35 A. Mahapatra, S. Sarkar, S. C. Biswas and K. Chattopadhyay, *Chem. Commun.*, 2019, **55**, 11052–11055.
36 N. Joshi, S. Basak, S. Kundu, G. De, A. Mukhopadhyay and K. Chattopadhyay, *Langmuir*, 2015, **31**, 1469–1478.
37 N. Taebnia, D. Morshedi, S. Yaghmaei, F. Aliakbari, F. Rahimi and A. Arpanaei, *Langmuir*, 2016, **32**, 13394–13402.
38 A. Mahapatra, S. Sarkar, S. C. Biswas and K. Chattopadhyay, ACS Chem, *Neurosci.*, 2020, **11**, 3442–3454.
39 M. Bopardikar, A. Bhattacharya, V. M. R. Kakita, K. Rachineni, L. C. Borde, S. Choudhary, S. R. K. Ainavarapu and R. V. Hosur, *RSC Adv.*, 2019, **9**, 28470–28477.
40 S. Honarmand, B. Dabirmanesh, M. Amanlou and K. Khajeh, *PLoS One*, 2019, **14**, e0217801.
41 M. T. Ardah, S. S. Ghanem, S. A. Abdulla, G. Lv, M. M. Emara, K. E. Paleologou, N. N. Vaikath, J.-H. Lu, M. Li, K. Vekrellis, D. Eliezer and O. M. A. El-Agnaf, *BMC Complementary Med. Ther.*, 2020, **20**, 73.
42 D. Morshedi, F. Aliakbari, A. Tayaranian-Marvian, A. Fassihi, F. Pan-Montojo and H. Pérez-Sánchez, *J. Food Sci.*, 2015, **80**, H2336–H2345.
43 H. Javed, M. F. Nagoor Meeran, S. Azimullah, A. Adem, B. Sadek and S. K. Ojha, *Front. Pharmacol.*, 2019, **9**, 1555.
44 A. Kakinen, I. Javed, A. Faridi, T. P. Davis and P. C. Ke, *Biochim. Biophys. Acta, Biomembr.*, 2018, **1860**, 1803–1809.
45 G. Bellomo, S. Bologna, L. Cerofolini, S. Paciotti, L. Gatticchi, E. Ravera, L. Parnetti, M. Fragai and C. Luchinat, *J. Phys. Chem. B*, 2019, **123**, 4380–4386.
46 B. M. Burmann, J. A. Gerez, I. Matečko-Burmann, S. Campioni, P. Kumari, D. Ghosh, A. Mazur, E. E. Aspholm, D. Šulskis, M. Wawrzyniuk, T. Bock, A. Schmidt, S. G. D. Rüdiger, R. Riek and S. Hiller, *Nature*, 2020, **577**, 127–132.
47 J. N. Rao, V. Dua and T. S. Ulmer, *Biochemistry*, 2008, **47**, 4651–4656.
48 R. Ahmed, J. Huang, D. K. Weber, T. Gopinath, G. Veglia, M. Akimoto, A. Khondker, M. C. Rheinstadter, V. Huynh, R. G. Wylie, J. C. Bozelli Jr, R. M. Epand and G. Melacini, *J. Am. Chem. Soc.*, 2020, **142**, 9686–9699.
49 M. T. Khan, I. Lampronti, D. Martello, N. Bianchi, S. Jabbar, M. S. Choudhuri, B. K. Datta and R. Gambari, *Int. J. Oncol.*, 2002, **21**, 187–192.
50 C. J. Yang, C. S. Wang, J. Y. Hung, H. W. Huang, Y. C. Chia, P. H. Wang, C. F. Weng and M. S. Huang, *Lung Cancer*, 2009, **66**, 162–168.
51 E. Nicolis, I. Lampronti, M. C. Dechecchi, M. Borgatti, A. Tamanini, N. Bianchi, V. Bezzerri, I. Mancini, M. G. Giri, P. Rizzotti, R. Gambari and G. Cabrini, *Int. Immunopharmacol.*, 2008, **8**, 1672–1680.
52 Y. F. Huang, S. L. Zhang, F. Jin, D. Cheng, Y. P. Zhou, H. R. Li, Z. M. Tang, J. Xue, W. Cai, J. H. Dong and L. Zhao, *Int. J. Immunopathol. Pharmacol.*, 2013, **26**, 85–92.
53 J. Moreira, L. C. Klein-Júnior, V. Cechinel Filho and F. de Campos Buzzi, *J. Ethnopharmacol.*, 2013, **146**, 318–323.
54 Y. J. Guo, L. Zhao, X. F. Li, Y. W. Mei, S. L. Zhang, J. Y. Tao, Y. Zhou and J. H. Dong, *Eur. J. Pharmacol.*, 2010, **635**, 79–86.
55 P. Li, R. Du, Y. Wang, X. Hou, L. Wang, X. Zhao, P. Zhan, X. Liu, L. Rong and Q. Cui, *Front. Microbiol.*, 2020, **11**, 182.
56 L. T. Lin, T. Y. Chen, S. C. Lin, C. Y. Chung, T. C. Lin, G. H. Wang, R. Anderson, C. C. Lin and C. D. Richardson, *BMC Microbiol.*, 2013, **13**, 1–15.
57 S. Shanmuganathan and N. Angayarkanni, *Vasc. Pharmacol.*, 2018, **108**, 23–35.
58 S. M. Hecht, D. E. Berry, L. J. MacKenzie, R. W. Busby and C. A. Nasuti, *J. Nat. Prod.*, 1992, **55**, 401–413.
59 R. Jakes, M. G. Spillantini and M. Goedert, *FEBS Lett.*, 1994, **345**, 27–32.
60 M. J. Volles and P. T. Lansbury Jr, *J. Mol. Biol.*, 2007, **366**, 1510–1522.
61 D. Marion, M. Ikura, R. Tschudin and A. Bax, *J. Magn. Reson.*, 1989, **85**, 393–399.
62 S. P. Skinner, R. H. Fogh, W. Boucher, T. J. Ragan, L. G. Mureddu and G. W. Vuister, *J. Biomol. NMR*, 2016, **66**, 111–124.
63 M. Biancalana and S. Koide, *Biochim. Biophys. Acta*, 2010, **1804**, 1405–1412.
64 M. R. Krebs, E. H. Bromley and A. M. Donald, *J. Struct. Biol.*, 2005, **149**, 30–37.
65 C. Xue, T. Y. Lin, D. Chang and Z. Guo, *R. Soc. Open Sci.*, 2017, **4**, 160696.
66 M. F. Bishop and F. A. Ferrone, *Biophys. J.*, 1984, **46**, 631–644.
67 M. D. Tuttle, G. Comellas, A. J. Nieuwkoop, D. J. Covell, D. A. Berthold, K. D. Kloepper, J. M. Courtney, J. K. Kim, A. M. Barclay, A. Kendall, W. Wan, G. Stubbs, C. D. Schwieters, V. Y. M. Lee, J. M. George and C. M. Rienstra, *Nat. Struct. Mol. Biol.*, 2016, **23**, 409–415.
68 B. Li, P. Ge, K. A. Murray, P. Sheth, M. Zhang, G. Nair, M. R. Sawaya, W. S. Shin, D. R. Boyer, S. Ye, D. S. Eisenberg, Z. H. Zhou and L. Jiang, *Nat. Commun.*, 2018, **9**, 1–10.
69 E. A. Mirecka, H. Shaykhalishahi, A. Gauhar, Ş. Akgül, J. Lecher, D. Willbold, M. Stoldt and W. Hoyer, *Angew. Chem., Int. Ed.*, 2014, **53**, 4227–4230.

70 E. D. Agerschou, P. Flagmeier, T. Saridaki, C. Galvagnion, D. Komnig, L. Heid, V. Prasad, H. Shaykhalishahi, D. Willbold, C. M. Dobson, A. Voigt, B. Falkenburger, W. Hoyer and A. K. Buell, *Elife*, 2019, **8**, e46112.
71 C. M. Cremers, D. Knoefler, S. Gates, N. Martin, J. U. Dahl, J. Lempart, L. Xie, M. R. Chapman, V. Galvan, D. R. Southworth and U. Jakob, *Mol. Cell*, 2016, **63**, 768–780.
72 H. T. Lam, M. C. Graber, K. A. Gentry and J. Bieschke, *Biochemistry*, 2016, **55**, 675–685.
73 T. Scheidt, U. Łapińska, J. R. Kumita, D. R. Whiten, D. Klenerman, M. R. Wilson, S. I. A. Cohen, S. Linse, M. Vendruscolo, C. M. Dobson, T. P. J. Knowles and P. Arosio, *Sci. Adv.*, 2019, **5**, eaau3112.
74 H. Shaykhalishahi, A. Gauhar, M. M. Wördehoff, C. S. Grüning, A. N. Klein, O. Bannach, M. Stoldt, D. Willbold, T. Hard and W. Hoyer, *Angew. Chem., Int. Ed.*, 2015, **54**, 8837–8840.
75 E. D. Agerschou, V. Borgmann, M. M. Wördehoff and W. Hoyer, *Chem. Sci.*, 2020, **11**, 11331–11337.
76 Z. A. Sorrentino, N. Vijayaraghavan, K. M. Gorion, C. J. Riffe, K. H. Strang, J. Caldwell and B. I. Giasson, *J. Biol. Chem.*, 2018, **293**, 18914–18932.
77 M. Terada, G. Suzuki, T. Nonaka, F. Kametani, A. Tamaoka and M. Hasegawa, *J. Biol. Chem.*, 2018, **293**, 13910–13920.
78 Z. A. Sorrentino, E. Hass, N. Vijayaraghavan, K. M. Gorion, C. J. Riffe, J. K. S. Dhillon and B. I. Giasson, *Neurosci. Lett.*, 2020, **732**, 135017.
79 K. P. Wu and J. Baum, *J. Am. Chem. Soc.*, 2010, **132**, 5546–5547.
80 X. Yang, B. Wang, C. L. Hoop, J. K. Williams and J. Baum, *Proc. Natl. Acad. Sci. U. S. A.*, 2021, **118**, e2017452118.
81 M. Vilar, H. T. Chou, T. Lührs, S. K. Maji, D. Riek-Loher, R. Verel, G. Manning, H. Stahlberg and R. Riek, *Proc. Natl. Acad. Sci. U. S. A.*, 2008, **105**, 8637–8642.